Task2 potassium channels set central respiratory CO_2 and O_2 sensitivity

Christian Gestreau[a,1], Dirk Heitzmann[b,c,1], Joerg Thomas[d,1], Véronique Dubreuil[e], Sascha Bandulik[b], Markus Reichold[b], Saïd Bendahhou[f], Patricia Pierson[f], Christina Sterner[b], Julie Peyronnet-Roux[a], Chérif Benfriha[a], Ines Tegtmeier[b], Hannah Ehnes[b], Michael Georgieff[d], Florian Lesage[g], Jean-Francois Brunet[e], Christo Goridis[e], Richard Warth[b,2,3], and Jacques Barhanin[f,2]

[a]Department of Neurovegetative Physiology, Centre National de la Recherche Scientifique, Université Paul Cézanne, 13397 Marseille, France; [b]Institute of Physiology, University of Regensburg, 93053 Regensburg, Germany; [c]Department of Internal Medicine, Nephrology and Rheumatology, University of Muenster, 48149 Muenster, Germany; [d]Department of Anaesthesiology, University of Ulm, 89075 Ulm, Germany; [g]Institut de Pharmacologie Moléculaire et Cellulaire, Centre National de la Recherche Scientifique, and Université de Nice Sophia Antipolis, 06560 Valbonne, France; [e]Département de Biologie, Ecole Normale Supérieure, Centre National de la Recherche Scientifique, 75005 Paris, France; and [f]Transport Ionique Aspects Normaux et Pathologiques, Centre National de la Recherche Scientifique, and Faculté des Sciences, Université de Nice Sophia Antipolis, 06108 Nice Cedex, France

Edited by Lily Y. Jan, University of California, San Francisco, CA, and approved December 14, 2009 (received for review September 3, 2009)

Task2 K^+ channel expression in the central nervous system is surprisingly restricted to a few brainstem nuclei, including the retrotrapezoid (RTN) region. All Task2-positive RTN neurons were lost in mice bearing a Phox2b mutation that causes the human congenital central hypoventilation syndrome. In plethysmography, *Task2*$^{-/-}$ mice showed disturbed chemosensory function with hypersensitivity to low CO_2 concentrations, leading to hyperventilation. Task2 probably is needed to stabilize the membrane potential of chemoreceptive cells. In addition, *Task2*$^{-/-}$ mice lost the long-term hypoxia-induced respiratory decrease whereas the acute carotid-body-mediated increase was maintained. The lack of anoxia-induced respiratory depression in the isolated brainstem–spinal cord preparation suggested a central origin of the phenotype. Task2 activation by reactive oxygen species generated during hypoxia could silence RTN neurons, thus contributing to respiratory depression. These data identify Task2 as a determinant of central O_2 chemoreception and demonstrate that this phenomenon is due to the activity of a small number of neurons located at the ventral medullary surface.

breathing | central chemoreceptors | K2P | KCNK5 | ventral medullary surface

Spontaneous breathing requires feedback controls in which detection of blood gases and pH is critical. At present, there is good understanding of the brainstem topology of respiratory centers, and functional measurements in vitro and in vivo have revealed the basic principles of the neuronal network required for respiratory rhythmogenesis and pattern generation. This network comprises several groups of respiratory neurons forming columns extending from the caudal ventrolateral medulla to the dorsolateral pons (1, 2). The activity of this network must be stable yet permanently adjusted to variations of O_2, CO_2, and pH during diverse physiological conditions, e.g., sleep, exercise, or high altitude (3). The precise physiological processes by which pH, CO_2, and O_2 changes are sensed and translated into the appropriate respiratory neural output are important mechanisms that are still a matter of debate (4, 5). Changes in arterial CO_2/pH are detected by peripheral chemoreceptors, mainly carotid bodies, and multiple chemoreceptive areas within the brainstem. Among the central chemoreceptive areas, two have attracted most attention: the raphe nuclei and the retrotrapezoid nucleus (RTN) (6, 7). The carotid bodies are the major sensors for acute O_2 changes. However, for longer periods of hypoxia, respiratory adaptation is substantially mediated by central mechanisms (8). The ventrolateral medullary surface comprising the RTN and the parafacial respiratory group (pFRG) has been proposed to contain intrinsically CO_2- and O_2-sensing neurons (9–12). Recently, a mouse model that carries a mutation of the transcription factor *Phox2b*, which causes congenital central hypoventilation syndrome in humans, was engineered. A specific loss of a population of *Phox2b*-expressing RTN/pFRG neurons was associated with early death of these newborn mice due to the lack of the ventilatory response to hypercapnia (13).

Among potential molecular targets that could be involved in chemosensitivity, K^+ channels that set the membrane potential are obvious candidates. Seventy-eight genes code for K^+ channels in mammals, but only a few of them produce currents that are reversibly blocked by hypoxia and by hypercapnia or acidification. Task1, -2, and -3 channels (gene nomenclature: KCNK3, KCNK5, and KCNK9) belong to a family of K^+ channels with four transmembrane segments and two pore domains (K_{2P} channels) (14). They produce background K^+ currents that are inhibited by external acidification and G-protein-coupled receptors (15) and activated by volatile anesthetics (16). Recent evidence suggesting that Task channels are inhibited by hypoxia comes from studies showing that the O_2-sensitive background K^+ currents in carotid-body type I cells have electrophysiological and pharmacological properties of Task1 and Task3 (17–19).

Task currents are also attractive candidates to mediate central chemoreception. Task1 and Task3 are expressed in multiple clusters of respiratory-related chemosensitive neurons, including the medullary raphe, RTN, pre-Bötzinger and Bötzinger complexes, lateral reticular nucleus, hypoglossal motoneurons, and locus coeruleus (20). Inhibition of Task currents by extracellular acidosis leads to depolarization and is expected to increase cell excitability and respiratory motoneuronal output. Moreover, volatile anesthetics were proposed to depress respiratory neurons through activation of Task channels, leading to hyperpolarization and neuronal silencing. However, a critical role of Task channels in central CO_2 chemosensitivity was questioned because the hypercapnic response persisted in double-mutant *Task1*$^{-/-}$/*Task3*$^{-/-}$ mice, although the chemosensitivity of raphe neurons, but not RTN neurons, was abolished (21).

Because no or only weak expression of Task2 has been found in the brain (22), this channel has not been considered for cen-

Author contributions: C. Gestreau, D.H., J.T., R.W., and J.B. designed research; C. Gestreau, D.H., J.T., V.D., S. Bandulik, M.R., S. Bendahhou, P.P., C.S., J.P.-R., C.B., I.T., H.E., F.L., J.-F.B., C. Goridis, R.W., and J.B. performed research; C. Gestreau, D.H., J.T., V.D., S. Bandulik, M. R., S. Bendahhou, C.S., I.T., H.E., R.W., and J.B. analyzed data; M.G. contributed new reagents/analytic tools; and C. Gestreau, C. Goridis, R.W., and J.B. wrote the paper.

The authors declare no conflict of interest.

This article is a PNAS Direct Submission.

[1]C. Gestreau, D.H., and J.T. contributed equally to this work.

[2]R.W. and J.B. shared last authorship.

[3]To whom correspondence should be addressed at: University Regensburg, Universitaetsstrasse 31, Regensburg 93053, Germany. E-mail: richard.warth@vkl.uni-regensburg.de.

This article contains supporting information online at www.pnas.org/cgi/content/full/0910059107/DCSupplemental.

tral chemoreception. Task2 has been described as an epithelial channel, abundant in kidney, salivary glands, and the colon. Recently, we showed that Task2 channels stabilize the HCO_3^- reabsorption in kidney proximal tubules and that, consequently, *Task2*-deficient mice present with metabolic acidosis (23). In addition, Task2 channels are involved in cell volume regulation (24–26).

Here, we show that *Task2* expression is restricted to a few brainstem nuclei in the mouse, including the ventral medullary surface, and is almost absent in other brain structures. In mice carrying a *Phox2b* mutation that causes the human congenital central hypoventilation syndrome (13), all Task2-positive RTN neurons were lost. In plethysmography and in vitro *en bloc* preparation, $Task2^{-/-}$ mice showed compromised central respiratory adaptation to hypoxia and hypercapnia. These data demonstrate that Task2 K^+ channels are important for the chemoreceptive properties of the respiratory network.

Results

Localization of Task2 in the Mouse Brainstem. The targeting vector used for the generation of $Task2^{-/-}$ mice contained a β-galactosidase gene (Lac-Z) (27). Surprisingly, specific labeling by the Lac-Z substrate X-gal was restricted to very few brainstem regions and was absent in other brain regions. In the medulla, staining was observed at the ventral medullary surface (VMS). It consisted of bilateral columns of cells extending over 1.5 mm, from 500 to 700 μm rostral to the obex up to the end of the facial motor nucleus. These cells formed clusters (>15 cells/hemisection) located within the marginal layer up to 100–300 μm deep in the parenchyma (Fig. 1 *A–E*). This region overlapped with the area corresponding to the RTN/pFRG. Task2-positive cells were observed along the brainstem surface ventral to the facial motor nucleus with highest densities at the caudal and rostral borders, in line with previous descriptions of pFRG (28) and RTN (29) neurons, respectively (Fig. 1 *A*, *D*, and *E*). No labeling was detected in the medial parapyramidal region of the VMS. In the pons, X-gal staining was restricted to the lateral superior olive (Fig. 1*C*) and the parvocellular reticular nucleus pars alpha (PCRtA) (Fig. 1*D*). In the rostral brainstem, dense clusters of labeled cells were observed in the dorsal raphe (DR) nucleus and in the intermediate lateral leminscus (Fig. 1*B*). A sparse labeling was present in the caudal inferior colliculus. No labeling was detected in the cervical spinal cord. The brainstem localization of Task2 is summarized in Fig. 1*F*.

Task2-Positive RTN Cells Are Missing in a Mouse Model for Congenital Central Hypoventilation Syndrome. The RTN contains glutamatergic neurons that are positive for the homeodomain transcription factor Phox2b. The role of Phox2b in the neural control of breathing was ushered in when mutations in Phox2b were discovered in humans associated with congenital central hypoventilation syndrome (CCHS) (30). CCHS is characterized by the failure of automatic control of breathing. Patients with CCHS do not exhibit signs of respiratory distress when challenged with hypercapnia or hypoxia. To model CCHS, the most frequent mutation, an expansion of a polyalanine stretch by seven residues, was introduced in mice (13). Transmitting chimeras produced heterozygous pups ($Phox2b^{+/27Ala}$) that died soon after birth from respiratory failure. Inspection of the hindbrain of $Phox2b^{+/27Ala}$ newborn mice showed that the RTN neurons, defined as Phox2b+/Vglut2+ cells located ventral and just caudal to the facial nucleus, were depleted by 85% (13). $Phox2b^{+/27Ala}$ male chimera were bred with $Task2^{-/-}$ females to produce $Task^{2+/-}$; $Phox2b^{+/27Ala}$ mice. As a spectacular result, the blue Task2-positive RTN neurons were absent in these mice, indicating that the population of neurons that express Task2 channels in the RTN overlap or represent a subpopulation of the set of RTN neurons known to be essential in respiratory chemosensitivity (Fig. 2).

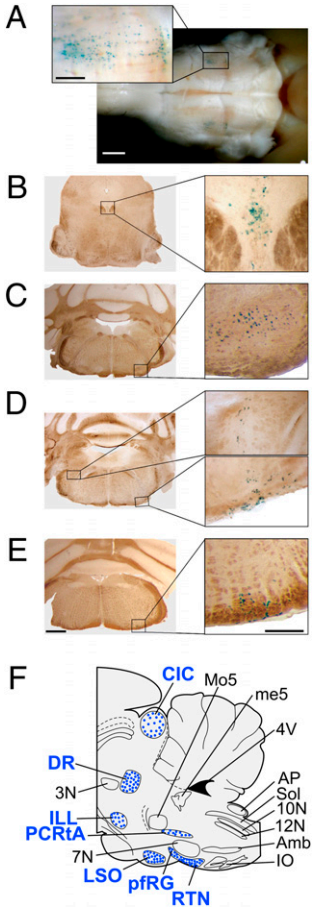

Fig. 1. Localization of Task2 channels in the adult mouse brainstem. (*A*) X-gal staining (blue) of the adult (6 months of age) mouse brainstem showing Task2-expressing cells at the ventral surface around the facial motor (VII) nucleus. The enlarged view (*Left Inset*) depicts labeled cells of the retrotrapezoid nucleus and parafacial respiratory group (RTN/pfRG). (*B–E*) Staining in coronal sections; dorsal is up. (*B*) Mesencephalon: X-gal–positive cells in the dorsal raphe nucleus. (*C*) Rostral pons: X-gal-positive cells in lateral superior olive. (*D*) Caudal pons, X-gal-positive cells at ventral surface (bottom inset) and in the parvocellular reticular formation pars alpha (PCRtA; top inset). (*E*) X-gal-positive cells at ventral medullary surface at the caudal end of the VII nucleus. (Scale bars: *Right* in *A* and *Left* in *B–E*: 1 mm; *Left Inset* of *A* and *Right Inset B–E*: 200 μm.) (*F*) Schematic of the brainstem (sagittal section) summarizing the distribution of Task2-expressing cells (blue dots) and their approximate rostrocaudal extension. 3N, oculomotor nucleus; 4V, fourth ventricle; 7N, facial nucleus; 10N, dorsal motor nucleus of vagus nerve; 12N, hypoglossal nucleus; Amb, ambiguus nucleus; AP, area postrema; CIC, central nucleus of the inferior colliculus; DR, dorsal raphe nucleus; ILL, intermediate nucleus of the lateral lemniscus; IO, inferior olive; LSO, lateral superior olive; me5, mesencephalic trigeminal tract; pfRG, parafacial respiratory group; PCRtA, parvicellular reticular nucleus, pars alpha; RTN, retrotrapezoid nucleus; Sol, nucleus of the solitary tract.

Acute Effects of Hypercapnia and Hypoxia on Breathing. The unique brainstem localization of Task2 suggested a role of this pH-regulated K^+ channel in the central chemosensitive control of breathing. Therefore, we investigated the respiratory response upon hypercapnia and hypoxia using whole-body plethysmography on unrestrained male mice. To reduce the contribution of peripheral chemoreceptors to the CO_2 response, hyperoxic hypercapnia was used instead of normoxic hypercapnia (31).

Under control conditions, main breathing parameters were similar in the two genotypes. However, the CO_2 response curve for $Task2^{-/-}$ mice was shifted to the left, with a threshold as low as 1%, instead of 3%, in wild type (Fig. 3 *A* and *B*). In wild-type mice,

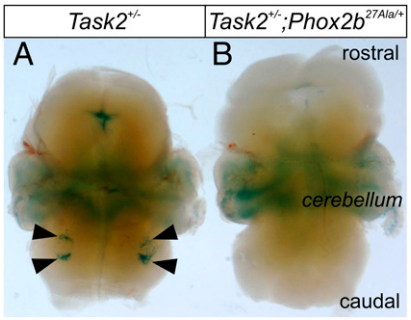

Fig. 2. Loss of Task2-positive cells in CCHS mouse embryo X-gal staining of brains (whole mount) of *Task2*$^{+/-}$ (*A*) and *Task2*$^{+/-}$; *Phox2b*$^{27Ala/+}$ (*B*) 15.5-day-old embryos. Task2-expressing RTN neurons (arrowheads) are present in *Task2*$^{+/-}$ (*A*) and specifically lost in *Phox2b*$^{27Ala/+}$, a mouse model for human congenital central hypoventilation syndrome (*B*). Meningeal Task2 staining is preserved in both types of embryos.

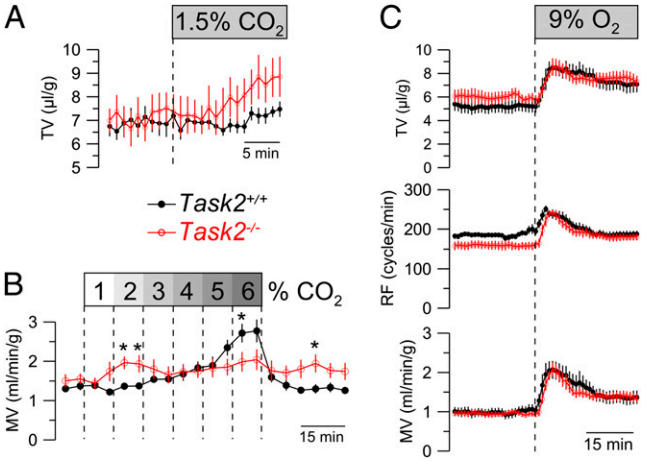

Fig. 3. Acute respiratory responses to hypercapnia and hypoxia. (*A* and *B*) Ventilation in response to inspiratory CO_2 was measured by plethysmography. Inspiratory gas was 100% O_2 or mixtures of O_2 and CO_2 as indicated. In comparison with *Task2*$^{+/+}$ ($n = 8$), *Task2*$^{-/-}$ mice ($n = 8$) were hypersensitive to small increases of CO_2. (*A*) The variations of tidal volume (TV) caused by 1.5% CO_2. (*B*) The variations of the minute volume (MV) at increasing CO_2 concentrations. (*C*) Acute responses to hypoxia (9% O_2) were not changed in *Task2*$^{-/-}$ ($n = 7$) versus *Task2*$^{+/+}$ ($n = 8$) mice. All animals were 3- to 6-month-old male mice. Symbols represent mean values ± SEM; $*P < 0.05$.

the response was biphasic. It increased linearly from 3% to 4% CO_2 followed by an abrupt and strong response at higher concentrations. Conversely, in *Task2*$^{-/-}$ mice, the minute volume (MV) reaches a maximum at 2% CO_2 and remains stable up to 6%. Superposition of the wild-type and knockout curves was observed between 3% and 5% CO_2. At higher CO_2 concentrations, *Task2*$^{-/-}$ mice had a smaller response than wild type. Reduction of the inspiratory O_2 concentration from 21% to 9% acutely increased respiration in both genotypes (Fig. 3*C*). This increase was transient, and respiration decreased again after a few minutes. The normal acute response to hypoxia suggested normal O_2 sensitivity of the chemoreceptive cells in carotid bodies.

Lack of Long-Term, Hypoxia-Induced Ventilatory Depression in *Task2*$^{-/-}$ Mice. Next, the response to long-term hypoxia was investigated at 8% O_2. This challenge produced substantial depression of respiration in wild-type animals (Fig. 4*A*). Hypoxic depression of MV was mainly caused by reduction of respiratory frequency (RF) and, to a lesser extent, by reduced tidal volume. This respiratory depression triggered by long-term hypoxia was absent in *Task2*$^{-/-}$ mice. To test the ventilatory acclimatization to chronic hypoxia (32), mice were kept under hypoxic conditions (10% O_2 corresponding to about 5,300 m altitude) for 20 h. During the first 3–4 h of hypoxia, wild-type animals exhibited profound respiratory depression of MV paralleled by prolongation of expiratory time (TE) and by a reduction of RF. This hypoxia-induced depression of respiration was followed by a phase of ventilatory acclimatization characterized by shortening of TE to reach control values after 10–12 h (Fig. 4 *B* and *C*). During the entire period of long-term hypoxia, ventilatory parameters remained unchanged in *Task2*$^{-/-}$ mice. Therefore, the respiratory phenotype of *Task2*$^{-/-}$ mice resembles that of wild-type mice after acclimatization to chronic hypoxia.

***En bloc* Preparations Confirm the Role of Task2 in Hypoxic Central Respiratory Adaptation.** Plethysmography showed abnormal respiratory response to hypoxia in *Task2*$^{-/-}$ mice. To further test for the central origin of this deficit, we used the rhythmic *en bloc* preparation of neonatal mouse brainstem, which retains the central chemoreceptors but is devoid of inputs from peripheral ones (Fig. 5 *A*–*C*). Basal RF was similar under control conditions in all genotypes. In wild-type and heterozygous mice, metabolic and respiratory acidosis induced increases in RF (about +40%), whereas metabolic alkalosis and anoxia significantly decreased RF (about −40%). *Task2*$^{-/-}$ mice exhibited similar responses to pH changes. However, the anoxia-induced depression was abolished in *Task2*$^{-/-}$ mice (Fig. 5 *D* and *E*). Detailed values of the *en bloc* preparation are shown in Table S1.

Discussion

We provide evidence that the pH-sensitive, two-pore-domain Task2 K^+ channel plays an important role in sensing hypercapnia and hypoxia. To this end, we have used an integrative approach combining whole-animal plethysmography, molecular histology, and in vitro *en bloc* experiments.

Task2 has been considered to be virtually absent in the central nervous system (22, 33). Using the Lac-Z-staining technique, Task2 localization was mapped in mouse brain. It showed a unique distribution restricted to a few brainstem areas and was undetectable in the forebrain. This finding contrasts with the wide CNS expression of the two other pH-sensitive Task1 and Task3 K^+ channels (34). In schematic terms, Task2 is expressed in four regions and only in a scattered manner. In mesencephalic sections, Task2 is found in the dorsal raphe nucleus and the lateral lemniscal region. In the pons, it is found in the dorsolateral column ending in the intertrigeminal region. With the exception of the dorsal raphe nucleus (6), these rostral brainstem areas have not been proposed to underlie central chemoreception. In the medulla oblongata, Task2 staining was observed only along the VMS in a zone corresponding to the RTN/pFRG. It has been shown that this region plays a key role in central chemoreception (3, 7, 9, 13, 35).

Exposure to hypoxia induces both ventilatory changes and a decrease in oxygen consumption (36). The hypoxia-induced ventilatory response is time-dependent, consisting of an immediate increase followed by depression of respiratory drive and further slow recovery upon long-term hypoxic exposure (8, 32). In plethysmography, *Task2*$^{-/-}$ mice exhibited a normal initial respiratory increase in response to hypoxia. Our results indicate that the peripheral chemoreflex arc is still intact in *Task2*$^{-/-}$ mice. Apparently, neither the O_2-sensing function of carotid bodies nor the central processing of afferent chemoreceptive inputs is dependent on the presence of Task2 channels. By contrast, the hypoxia-induced depression of respiration is abolished in *Task2*$^{-/-}$ mice. It has been proposed that this phase of the hypoxic response reflects inhibitory mechanisms located in the VMS (8, 9, 37). Our data suggest that Task2 is a key molecular substrate of hypoxic ventilatory depression. During long-term

PHYSIOLOGY

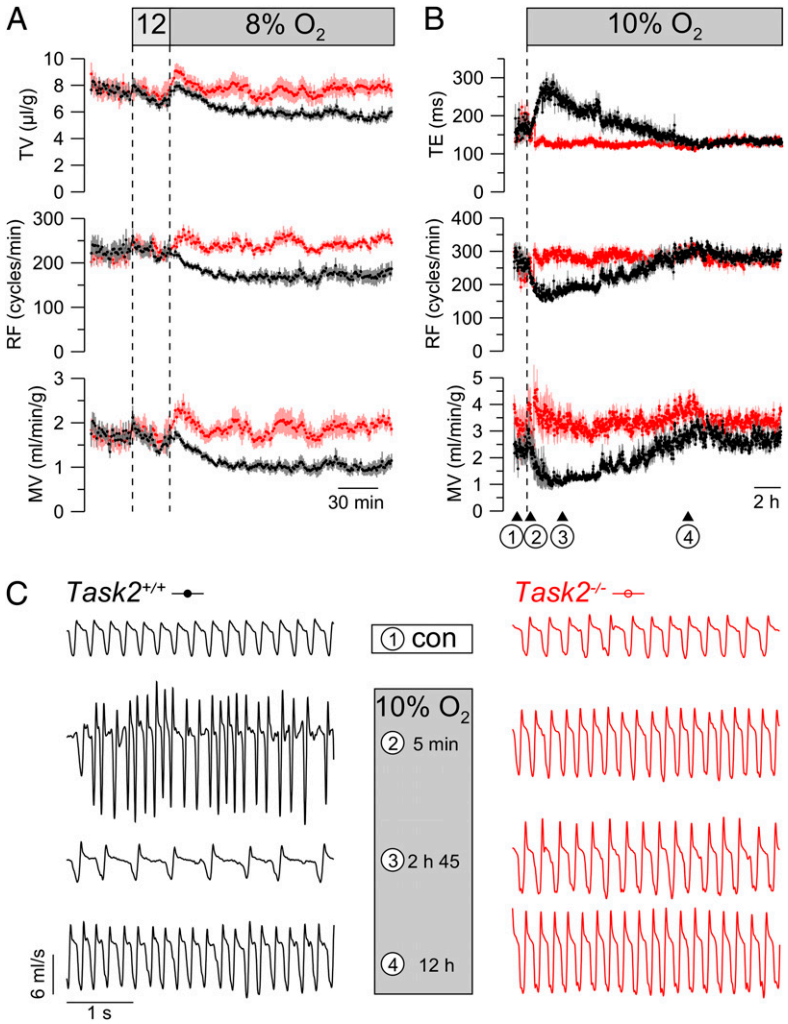

Fig. 4. Hypoxia-induced respiratory depression and adaptation to chronic hypoxia. (*A*) In plethysmography, *Task2*$^{+/+}$ mice (n = 8) showed depression of respiration during prolonged severe hypoxia (12% followed by 8% O_2), which was virtually absent in *Task2*$^{-/-}$ (n = 8). Tidal volume (TV), respiratory frequency (RF), and minute volume (MV) are shown. (*B*) After several hours of hypoxia, *Task2*$^{+/+}$ mice showed acclimatization to long-term hypoxia: *Task2*$^{+/+}$ mice (n = 6) slowly recovered from the hypoxia-induced prolongation of the expiratory time (TE) leading to a rise in RF. No changes of respiratory parameters were observed during 20 h exposure to hypoxia in *Task2*$^{-/-}$ mice (n = 6). (*C*) Original flow traces of individual animals at various time points (1–4) as indicated in *B*. All animals were 3- to 6-month-old male mice.

hypoxia, hypoxic depression is followed by a phase of acclimatization during which breathing slowly increases (32). This acclimatization phase was consistently observed in wild-type mice but was strongly diminished or absent in Task2$^{-/-}$ mice. This suggests that hypoxic depression in wild-type animals was caused by activation of Task2 channels. Then, their progressive closure led to acclimatization, i.e., to a slow increase in respiration. In *Task2*$^{-/-}$ mice, there is no depression (no activation of Task2 possible) and hence no acclimatization. The possibility of a transcriptional Task2 regulation being the mechanism underlying this process was excluded by quantitative PCR experiments (Fig. S1, *SI Results*).

Task2 K^+ channels are expressed in a variety of peripheral tissues, including the kidney where they play a role in bicarbonate reabsorption and pH balance (23). To eliminate the possibility that the lack of hypoxic depression of respiration in *Task2*$^{-/-}$ mice is simply due to the resulting metabolic acidosis, an equivalent blood acidification was elicited in wild-type mice using ammonium chloride in the drinking water (Fig. S2, *SI Results*). This treatment did not suppress the hypoxic hypoventilation, indicating that metabolic acidosis, which potentially prevents respiratory alkalosis, does not account for the observed knockout phenotype. During metabolic acidosis, *Task2*$^{+/+}$ mice exhibited slight changes in the CO_2 response but did not produce strong responses at 1% and 2% CO_2 as was observed in *Task2*$^{-/-}$ animals (Fig. 3 and Fig. S2, *SI Results*). In conclusion, the slight metabolic acidosis of *Task2*$^{-/-}$ mice probably has a modulating effect on chemosensitivity, but it does not explain the suppression of hypoxic hypoventilation and the strong response to very low CO_2 concentrations.

The *en bloc* brainstem–spinal cord preparation can be considered as a minimum functional respiratory network capable of generating rhythmic activity (1). The pons was discarded in the mouse preparation because it prevents the rhythmic activity probably due to inhibitory inputs (38). Thus, this preparation reflects phrenic activity driven by a neuronal network reduced to medullary structures. In wild-type mice, superfusion with anoxic fluid induced a drastic and reversible reduction of the respiratory frequency as observed by others (9, 39–41). In agreement with plethysmographic results, this effect was abolished in *Task2*$^{-/-}$ mice. Therefore, in vitro experiments have identified Task2 as a factor necessary for medullary hypoxia sensitivity. Furthermore, because the *en bloc* preparation retains only the RTN/pFRG region as a Task2-expressing structure, the lack of hypoxia sen-

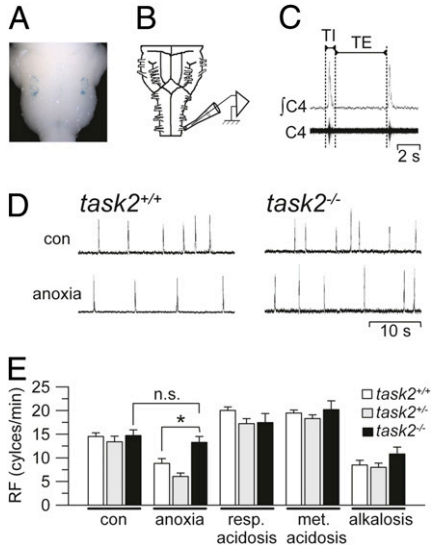

Fig. 5. Brainstem *en bloc* preparation of newborn mice. (*A*) Task2 X-gal staining of the RTN cells of the neonatal brainstem. (*B*) Schematic of the *en bloc* preparation that retains medullary structures and the caudal-most aspect of the pons. A suction electrode is placed on the fourth cervical roots (C4) to record rhythmic respiratory-like activity. (*C*) Example of raw (C4) and integrated (∫C4) inspiratory bursts from which the respiratory frequency is measured as well as the amplitude, surface, and duration of the inspiratory (TI) and expiratory (TE) phases. (*D*) Comparison of respiratory activity in *Task2*$^{+/+}$ and *Task2*$^{-/-}$ mice during control (con) and after 5 min of anoxic conditions (anoxia). Note the lack of hypoxic frequency decline in the *Task2*$^{-/-}$ mouse. (*E*) Effects of anoxia, respiratory acidosis, metabolic acidosis, and alkalosis on respiratory frequency (RF) (*task2*$^{+/+}$: $n = 10$; *Task2*$^{+/-}$: $n = 8$; *Task2*$^{-/-}$: $n = 7$). *$P < 0.05$.

sitivity at least in this in vitro preparation can be attributed to this particular region of the VMS.

Classically, the acclimatization to sustained hypoxia is thought to involve changes in the CO_2 sensitivity of breathing (42). RTN neurons are responsive to CO_2, are glutamatergic, and have axonal projections anatomically appropriate for driving the respiratory network (43, 44). Analysis of the hypercapnic response at different CO_2 concentrations revealed that *Task2*$^{-/-}$ mice were hypersensitive to low CO_2 concentrations and showed an attenuated response at high CO_2 values. Displaying a lack of hypoxic depression and this CO_2 phenotype, *Task2*$^{-/-}$ mice behaved like animals acclimatized to low O_2 levels.

The respiratory phenotype of the *Task2*$^{-/-}$ mice is characterized by the lack of hypoxic ventilatory depression, which goes along with the resetting of the CO_2 sensitivity in vivo and the absence of the anoxic response in the *en bloc* brainstem preparation. These observations are in good agreement with the localization of Task2 channels in RTN neurons, which have been implicated in the central respiratory chemo-adaptation. The elevation of blood CO_2 likely depolarizes RTN neurons by closing pH-sensing K^+ channels. Until recently, Task1 and Task3 pH-sensitive K^+ channels were thought to underlie this K^+ conductance of RTN neurons. A recent study using double *Task1/3* knockout mice failed to confirm this hypothesis (21). In contrast, our results suggest that Task2 channels contribute to the hyperpolarizing K^+ conductance of RTN neurons. We hypothesize that Task2 currents keep the membrane hyperpolarized to prevent a respiratory increase at low CO_2 concentrations and that the strong ventilatory drive observed at CO_2 concentrations above 5% may be caused by their closure. In the absence of Task2, already low CO_2 concentrations lead to relevant depolarization and cause increased CO_2 sensitivity. This hypothesis implies that Task2 is not the sole, and probably not the main, pH/CO_2 sensor but is implicated in setting the threshold of the pH/CO_2 response. For example, Kir currents have been described to be inhibited by CO_2-induced acidification in RTN neurons (41). In *Phox2b*$^{+/27Ala}$ mice, there is not only loss of Task2 expression, but also massive depletion of RTN neurons, which explains the complete absence of the CO_2 response, which in turn leads to death of these mice during the newborn period.

The *en bloc* experiments suggest that hypoxia hyperpolarizes RTN neurons directly through activation of Task2 channels, thereby inducing a respiratory frequency decline. Reactive oxygen species (ROS), which are generated during hypoxia (45), activate hTASK2 channels (Fig. S3, *SI Results*) (26, 46). Therefore, ROS generation in RTN neurons is a possible hypothesis to interpret the hypoxia-induced activation of Task2. Taken together, the Task2 channel activity appears to be an important determinant for the intact CO_2 and O_2 chemosensitivity. However, our experimental evidence is still a rather global one. Future electrophysiological recordings of RTN neurons will provide important insights into the exact role of Task2 for central chemosensitivity.

In recent years, the RTN/pfRG region has attracted considerable interest for its role in the control of respiratory rhythmogenesis and its modulation by central chemoreception. The neuropil of this region has a high degree of complexity, suggesting that chemosensitive cells are regulated by diverse neurochemical inputs. In addition, this region sends efferent projections toward multiple brainstem nuclei involved in the coordination of the cardio-respiratory function. In future studies, the characterization of the Task2-positive neurons and their function in chemoreception will certainly provide unique insights into the complex control of vital functions (47).

Defects in central chemoreception associated with impaired breathing are responsible for several human pathologies such as central sleep apnea, periodic breathing in high altitude, sudden infant death syndrome, and CCHS. Recently, most RTN neurons were found to be absent in a CCHS mouse model. The finding that this neuronal population includes the Task2-positive RTN neurons further emphasizes the likely role of this channel in chemosensitivity. The pharmacological modulation of Task2 channels could provide a previously undescribed therapeutic strategy for central respiratory diseases.

Materials and Methods

Animals. The *Task2* knockout (*Task2*$^{-/-}$) mouse was generated by exon trapping techniques using the vector pGTOTMpf containing LacZ and placental alkaline phosphatase marker genes (27). The *Task2*$^{-/-}$ mouse was kindly provided by K. Mitchell and W. C. Skarnes (University of California, Berkeley). Animals were backcrossed into the C57BL6 genetic background for 10 generations. They were kept on a standard diet with free excess to chow and water. The experimental protocols were approved by the local councils for animal care and were conducted according to German and French laws for animal care.

Plethysmography. A whole-body plethysmographic device for unrestrained animals (EMKA Technologies) was used to measure ventilation parameters of male mice (3–6 months of age). Data were registered and analyzed with IOX software (EMKA Technologies). Values were averaged over 1 min. Hypoxia and hypercapnia were achieved by a mixture of variable concentrations of O_2, CO_2, and N_2 in the air supply. With the use of whole-body plethysmography in small rodents, the volume signal can be confounded with gas rarefaction/compression related to airway resistance and rapid airflow. This is a necessary caveat in applying this very useful method.

Histology. Heterozygous mice anesthetized with isoflurane were perfused via the abdominal aorta with 50 mL of PBS (0.1 M, pH 7.4) followed by 3% paraformaldehyde solution. Cryosections (40 μm) of brainstem and cervical spinal cord were stained with X-gal for 24 h as previously described (23). Every two to four sections were processed for X-gal staining. Alternate sections were counterstained with cresyl–violet to delineate anatomical structures.

In Vitro *en Bloc* Preparation of Neonatal Mouse Brainstem. The brainstem and cervical spinal cord were isolated from halothane anesthetized newborn C57BL/6 mice (0–3 d), and recordings were performed as described (48). The

PHYSIOLOGY

pons was eliminated by transection of the brainstem at the level of the sixth cranial nerve roots (48). The control artificial cerebrospinal fluid (aCSF) solution (in mmol/L: NaCl 124, KCl 5, KH_2PO_4 1.2, $CaCl_2$ 2.4, $MgSO_4$ 1.3, $NaHCO_3$ 26, glucose 30, pH 7.4) was equilibrated with 95% O_2 and 5% CO_2, warmed to 27° C. Hypercapnic acidic aCSF equilibrated with 8% CO_2 (pH 7.2) was used as a model for respiratory acidosis; normocapnic acidic aCSF containing 13 mM HCO_3^- (pH 7.2) was used as a model for metabolic acidosis; normocapnic alkaline aCSF containing 52 mM HCO_3^- (pH 7.8) was used as a model for metabolic alkalosis; and, for very low O_2 conditions, aCSF was equilibrated with 95% N_2 and 5% CO_2 (anoxic aCSF, pH 7.4). Inspiratory discharges of the phrenic efferent fibers were recorded from C4 ventral roots with glass-suction electrodes. Raw electrical activities were amplified, filtered (50 Hz–5 kHz), fed into a leaky integrator (time constant 100 ms), and analyzed (System3, TDT and MATLAB software; NeuroExplorer, Plexon). The respiratory frequency was defined as the frequency of the spontaneous rhythmic C4 bursts. Integrated C4 activities were used to measure the duration of the inspiratory burst (Ti) and its amplitude and surface area. Control values were determined during the 10 min preceding the test, and respiratory parameters were averaged over successive 5-min periods during the test. After stabilization of the preparation, C4 output was measured for 15 min in each of the test solutions (separated by 15 min control aCSF). Test solutions were applied in a sequential order that was randomized to avoid time-dependent effects.

Statistics. Data are shown as mean values ± SEM from *n* observations. Paired as well as unpaired Student's *t* test was used as appropriate. Data from in vitro *en bloc* experiments were compared by analysis of variance with repeated measures (Statview; SAS Institute) followed by Fisher's Protected Least Significant Difference correction for multiple comparisons. Differences were considered significant if $P < 0.05$.

ACKNOWLEDGMENTS. The authors thank Dr. K. Mitchell and Prof. Dr. W. Skarnes for generously providing the *Task2*$^{-/-}$ mice; M. M. Larroque for the expert assistance; Dr. Patrick Sanchez for his involvement in signal treatment and software programming; and Prof. Dr. M. Gassmann, Dr. Jorge Soliz, and Dr. Isabelle Arrighi for technical support. The study was supported by the Deutsche Forschungsgemeinschaft (SFB699 and FOR1086 to R.W.), by the Centre National de la Recherche scientifique, and by Provence-Alpes-Côte d'Azur Region (C. Gestreau and J.B.).

1. Richter DW, Spyer KM (2001) Studying rhythmogenesis of breathing: Comparison of in vivo and in vitro models. *Trends Neurosci* 24:464–472.
2. Feldman JL, Del Negro CA (2006) Looking for inspiration: New perspectives on respiratory rhythm. *Nat Rev Neurosci* 7:232–242.
3. Feldman JL, Mitchell GS, Nattie EE (2003) Breathing: rhythmicity, plasticity, chemosensitivity. *Annu Rev Neurosci* 26:239–266.
4. Putnam RW, Filosa JA, Ritucci NA (2004) Cellular mechanisms involved in CO(2) and acid signaling in chemosensitive neurons. *Am J Physiol Cell Physiol* 287:C1493–C1526.
5. Jiang C, Rojas A, Wang R, Wang X (2005) CO2 central chemosensitivity: Why are there so many sensing molecules? *Respir Physiol Neurobiol* 145:115–126.
6. Severson CA, Wang W, Pieribone VA, Dohle CI, Richerson GB (2003) Midbrain serotonergic neurons are central pH chemoreceptors. *Nat Neurosci* 6:1139–1140.
7. Guyenet PG, Stornetta RL, Bayliss DA (2008) Retrotrapezoid nucleus and central chemoreception. *J Physiol* 586:2043–2048.
8. Vizek M, Pickett CK, Weil JV (1987) Biphasic ventilatory response of adult cats to sustained hypoxia has central origin. *J Appl Physiol* 63:1658–1664.
9. Voituron N, Frugière A, Champagnat J, Bodineau L (2006) Hypoxia-sensing properties of the newborn rat ventral medullary surface in vitro. *J Physiol* 577:55–68.
10. Lahiri S, Forster RE II (2003) CO2/H(+) sensing: Peripheral and central chemoreception. *Int J Biochem Cell Biol* 35:1413–1435.
11. Robbins PA (2001) Is ventilatory acclimatization to hypoxia a phenomenon that arises through mechanisms that have an intrinsic role in the regulation of ventilation at sea level? *Adv Exp Med Biol* 502:339–348.
12. Nattie E, Li A (2009) Central chemoreception is a complex system function that involves multiple brain stem sites. *J Appl Physiol* 106:1464–1466.
13. Dubreuil V, et al. (2008) A human mutation in Phox2b causes lack of CO2 chemosensitivity, fatal central apnea, and specific loss of parafacial neurons. *Proc Natl Acad Sci USA* 105:1067–1072.
14. Lesage F, Lazdunski M (2000) Molecular and functional properties of two-pore-domain potassium channels. *Am J Physiol Renal Physiol* 279:F793–F801.
15. Mathie A (2007) Neuronal two-pore-domain potassium channels and their regulation by G protein-coupled receptors. *J Physiol* 578:377–385.
16. Patel AJ, Honoré E (2001) Properties and modulation of mammalian 2P domain K+ channels. *Trends Neurosci* 24:339–346.
17. Kim D, Cavanaugh EJ, Kim I, Carroll JL (2009) Heteromeric TASK-1/TASK-3 is the major oxygen-sensitive background K+ channel in rat carotid body glomus cells. *J Physiol* 587:2963–2975.
18. Buckler KJ, Williams BA, Honore E (2000) An oxygen-, acid- and anaesthetic-sensitive TASK-like background potassium channel in rat arterial chemoreceptor cells. *J Physiol* 525:135–142.
19. Weir EK, López-Barneo J, Buckler KJ, Archer SL (2005) Acute oxygen-sensing mechanisms. *N Engl J Med* 353:2042–2055.
20. Sirois JE, Lei Q, Talley EM, Lynch C, III, Bayliss DA (2000) The TASK-1 two-pore domain K+ channel is a molecular substrate for neuronal effects of inhalation anesthetics. *J Neurosci* 20:6347–6354.
21. Mulkey DK, et al. (2007) TASK channels determine pH sensitivity in select respiratory neurons but do not contribute to central respiratory chemosensitivity. *J Neurosci* 27: 14049–14058.
22. Reyes R, et al. (1998) Cloning and expression of a novel pH-sensitive two pore domain K^+ channel from human kidney. *J Biol Chem* 273:30863–30869.
23. Warth R, et al. (2004) Proximal renal tubular acidosis in TASK2 K+ channel-deficient mice reveals a mechanism for stabilizing bicarbonate transport. *Proc Natl Acad Sci USA* 101:8215–8220.
24. Niemeyer MI, Cid LP, Barros LF, Sepúlveda FV (2001) Modulation of the two-pore domain acid-sensitive K^+ channel TASK-2 (KCNK5) by changes in cell volume. *J Biol Chem* 276:43166–43174.
25. Barriere H, et al. (2003) Role of TASK2 potassium channels regarding volume regulation in primary cultures of mouse proximal tubules. *J Gen Physiol* 122:177–190.
26. L'Hoste S, et al. (2007) Role of TASK2 in the control of apoptotic volume decrease in proximal kidney cells. *J Biol Chem* 282:36692–36703.
27. Mitchell KJ, et al. (2001) Functional analysis of secreted and transmembrane proteins critical to mouse development. *Nat Genet* 28:241–249.
28. Onimaru H, Ikeda K, Kawakami K (2008) CO_2-sensitive preinspiratory neurons of the parafacial respiratory group express Phox2b in the neonatal rat. *J Neurosci* 28: 12845–12850.
29. Takakura AC, et al. (2008) Selective lesion of retrotrapezoid Phox2b-expressing neurons raises the apnoeic threshold in rats. *J Physiol* 586:2975–2991.
30. Amiel J, et al. (2003) Polyalanine expansion and frameshift mutations of the paired-like homeobox gene PHOX2B in congenital central hypoventilation syndrome. *Nat Genet* 33:459–461.
31. Rodman JR, Curran AK, Henderson KS, Dempsey JA, Smith CA (2001) Carotid body denervation in dogs: Eupnea and the ventilatory response to hyperoxic hypercapnia. *J Appl Physiol* 91:328–335.
32. Powell FL, Milsom WK, Mitchell GS (1998) Time domains of the hypoxic ventilatory response. *Respir Physiol* 112:123–134.
33. Medhurst AD, et al. (2001) Distribution analysis of human two pore domain potassium channels in tissues of the central nervous system and periphery. *Brain Res Mol Brain Res* 86:101–114.
34. Talley EM, Solorzano G, Lei Q, Kim D, Bayliss DA (2001) Cns distribution of members of the two-pore-domain (KCNK) potassium channel family. *J Neurosci* 21:7491–7505.
35. Mitchell RA, Loeschcke HH, Massion WH, Severinghaus JW (1963) Respiratory responses mediated through superficial chemosensitive areas on the medulla. *J Appl Physiol* 18:523–533.
36. Mortola JP, Saiki C (1996) Ventilatory response to hypoxia in rats: Gender differences. *Respir Physiol* 106:21–34.
37. Bodineau L, Cayetanot F, Frugière A (2001) Fos study of ponto-medullary areas involved in the in vitro hypoxic respiratory depression. *Neuroreport* 12:3913–3916.
38. Hilaire G, Viemari JC, Coulon P, Simonneau M, Bévengut M (2004) Modulation of the respiratory rhythm generator by the pontine noradrenergic A5 and A6 groups in rodents. *Respir Physiol Neurobiol* 143:187–197.
39. Okada Y, Kawai A, Mückenhoff K, Scheid P (1998) Role of the pons in hypoxic respiratory depression in the neonatal rat. *Respir Physiol* 111:55–63.
40. Voituron N, Frugière A, Gros F, Macron JM, Bodineau L (2005) Diencephalic and mesencephalic influences on ponto-medullary respiratory control in normoxic and hypoxic conditions: An in vitro study on central nervous system preparations from newborn rat. *Neuroscience* 132:843–854.
41. Kawai A, Onimaru H, Homma I (2006) Mechanisms of CO2/H+ chemoreception by respiratory rhythm generator neurons in the medulla from newborn rats in vitro. *J Physiol* 572:525–537.
42. León-Velarde F, Richalet JP (2006) Respiratory control in residents at high altitude: Physiology and pathophysiology. *High Alt Med Biol* 7:125–137.
43. Mulkey DK, et al. (2004) Respiratory control by ventral surface chemoreceptor neurons in rats. *Nat Neurosci* 7:1360–1369.
44. Weston MC, Stornetta RL, Guyenet PG (2004) Glutamatergic neuronal projections from the marginal layer of the rostral ventral medulla to the respiratory centers in rats. *J Comp Neurol* 473:73–85.
45. Mironov SL, Langohr K (2007) Modulation of synaptic and channel activities in the respiratory network of the mice by NO/cGMP signalling pathways. *Brain Res* 1130: 73–82.
46. Lee YM, et al. (2006) NOX4 as an oxygen sensor to regulate TASK-1 activity. *Cell Signal* 18:499–507.
47. Rosin DL, Chang DA, Guyenet PG (2006) Afferent and efferent connections of the rat retrotrapezoid nucleus. *J Comp Neurol* 499:64–89.
48. Hilaire G, Bou C, Monteau R (1997) Rostral ventrolateral medulla and respiratory rhythmogenesis in mice. *Neurosci Lett* 224:13–16.